Vol. 34 (2003) *ACTA PHYSICA POLONICA B* No 10

FINITE TEMPERATURE LATTICE QCD*

E. Laermann

Fakultät für Physik, Universität Bielefeld
33501 Bielefeld, Germany

(Received August 5, 2003)

The article presents a selected set of recent results from numerical investigations of QCD at finite temperature. It is focused *(i)* on the present understanding of thermodynamic properties of QCD in the presence of dynamical quarks at various masses and at small yet phenomenologically relevant values for the baryon density and *(ii)* on a fairly new approach to studying thermal hadronic excitations.

PACS numbers: 05.70.Ce, 11.15.Ha, 12.38.Gc

1. Introduction

Understanding the properties of elementary particles at high temperature and density is one of the major goals of contemporary physics. This purpose is served by the running, commissioned and planned heavy ion accelerators. On the theory side, much information has been delivered by numerical simulations of lattice QCD. Static-equilibrium physics is well under control in the continuum limit for the pure gauge theory without quarks. Calculations with dynamical quarks are currently limited, with some exceptions, to pion masses $m_\pi \simeq 300$ MeV and are still affected by lattice cutoff effects. Nevertheless, results on the critical temperature, the phase diagram and the equation of state are becoming reliable quantitatively due to the use of so-called improved actions which reduce the discretization effects. Moreover, the systematic errors can and will be reduced in future computations. Beyond that, considerable progress has been made recently in the problem of studying QCD at non-vanishing chemical potential and in addressing real-time properties at finite temperature QCD. These advances are in the focus of this contribution.

* Presented at the Workshop on Random Geometry, Kraków, Poland, May 15–17, 2003.

2. Thermodynamics

Full QCD, *i.e.* strong interactions in the presence of dynamical quarks, is expected to have a rich phase diagram depending crucially on the values of quark masses and chemical potentials corresponding to baryon densities of various flavor. Expectations on the phase diagram are mostly borne out off studies of σ-models with, presumably, the same global symmetries as relevant for QCD in the vicinity of the phase transition to the plasma phase where long range correlations dominate the dynamical behavior. These expectations [1, 2] are summarized in Fig. 1 in the plane of degenerate u- and d-quark masses and an independent value for the strange quark mass.

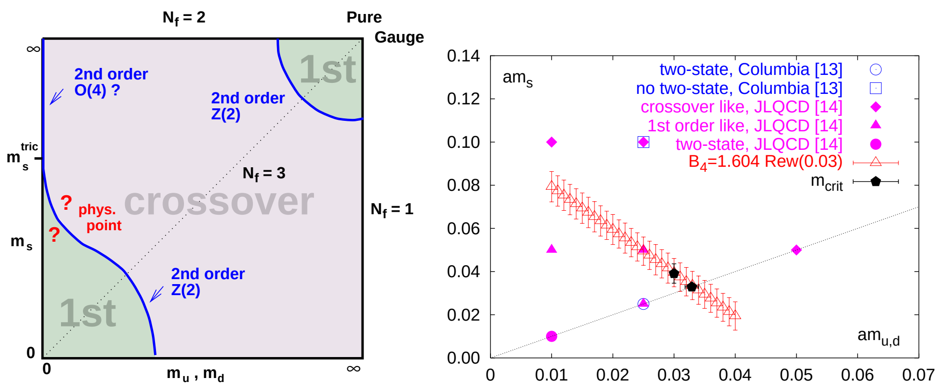

Fig. 1. Expectations (left) and results (right) on the phase diagram in the plane of degenerate u- and d-quark and strange quark masses. (The right plot is from [12].)

For instance, in the limit of infinitely heavy (static) quarks the transition is of first order and in the class of a (three-dimensional) Z(3) Potts model. The region of first order transitions ends in a critical (second order) line with the nature of a Z(2) Ising model [2].

For two massless flavors one generally expects a second order chiral transition with O(4) behavior. This is subject to the effective restoration of the (triangle) $\mathrm{U}_A(1)$ anomaly: if topologically non-trivial gauge field configurations have died out sufficiently at the chiral transition temperature the two flavor transition would be first order [1]. The current lattice understanding is that they have not [3], correspondingly all indications point to a continuous behavior at the critical temperature — yet, evidence for a critical O(4) behavior is not universal [4–8]. Since this problem is related to continuum symmetries being fully respected on the lattice further progress depends on either being able to carry out the continuum limit prior to the chiral one or finding lattice actions with improved chiral properties which are tractable numerically. Much work has been devoted to the latter approach recently [9].

For three massless flavors the transition most likely is first order. Expectations and lattice results agree on that. The region of first order transitions will end in a critical line. QCD on that line is expected to be in the three-dimensional Z(2) class [2] which has been supported by lattice simulations recently [10].

With this knowledge it becomes somewhat easier to follow the line in the plane of non-degenerate masses, either by direct simulations at appropriate mass values or by reweighting in the quark mass. The present understanding based on simulations with standard staggered discretizations is shown in Fig. 1. In physical units, the critical end point for three degenerate quarks lies at a pion mass of about 300 MeV [10, 11]. Assuming that the slope of the line is correctly approximated by the reweighting method [12] — with some support from the data points coming from direct simulation [12–14] — the ratio of critical strange to physical u-quark mass of $m_s^{\rm crit}/m_u^{\rm phys} \simeq 10$ would already be too small for QCD at the realized mass values being first order [12]. This becomes even more unlikely in view of the observation that the three-flavor critical end point moves to pion masses considerably less than 200 MeV in a computation based on an improved fermion action *i.e.* an action which leads to smaller discretization effects.

Critical temperatures, at least for degenerate quarks are known somewhat longer [15–20]. In the chiral limit $T_{\rm c}$ amounts to 175(5) MeV for two flavors [15, 17] and is, quite independent of the quark mass, about 20 MeV lower for three [15]. Again, these numbers originate from coarse lattices, however, improved actions have been used and, moreover, there is agreement in the two-flavor case between Wilson [17] and staggered [15] discretizations.

Much progress has been achieved in numerical studies of QCD at non-vanishing baryon density or chemical potential $\mu_B = 3\mu_q$. At $\mu_q \neq 0$ the action becomes complex and Monte Carlo simulations are not possible. Reweighting zero temperature $\mu_q = 0$ configurations to finite μ_q fails [21]. The new approaches are less ambitious insofar they are limited to μ_q values which are small but phenomenologically interesting as they are in the range important for RHIC physics [22], $\mu_B \simeq 50$ MeV. The three different techniques being used are *(i)* multiparameter reweighting [23, 24] from $\mu_q = 0$ configurations at $T \simeq T_{\rm c}$, *(ii)* analytic continuation [25, 26] of results at imaginary μ_q where simulations are possible [27] and *(iii)* Taylor expansion [28–31] around $\mu_q = 0$. These ways, the critical temperature $T_{\rm c}(\mu_q)$ was mapped out as a function of the chemical potential for $N_F = 2$ [25, 30], $N_F = 2+1$ [24] and $N_F = 4$ [26]. In [24] also the location of the critical end-point was estimated. Where comparisons are possible reasonable agreement was found. Some results are shown in Fig. 2. As such, they suggest that the deviation of $T_{\rm c}$ from its value at $\mu_B = 0$ is small at RHIC. Moreover, there

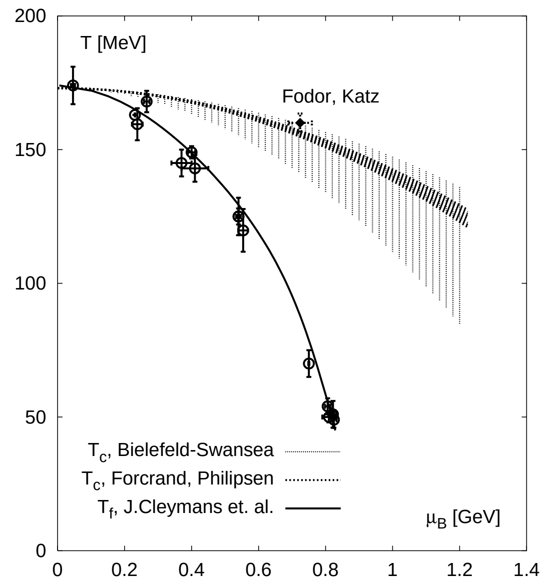

Fig. 2. The critical temperature as a function of the chemical potential $\mu_B = 3\mu_q$ [25, 30]. $T_{\rm f}$ is the chemical freeze-out temperature obtained from fitting statistical models to particle ratios measured at various heavy ion collision experiments [32]. Also shown is the estimate of the critical end-point [24].

seems to be a large region in the (μ_B, T) plane where the chemical freeze-out temperature $T_{\rm f}$ from statistical models [32] is considerably lower than the critical temperature which would leave interesting experimental options.

The techniques mentioned in the last paragraph have also been used to compute the pressure at non-vanishing chemical potential [33, 34]. For instance, in the Taylor expansion approach, the difference to the pressure at vanishing μ_q is expressed as a series in the fugacity μ_q/T,

$$\Delta\left(\frac{p}{T^4}(\mu_q)\right) = \frac{p}{T^4}\bigg|_{\mu_q} - \frac{p}{T^4}\bigg|_{\mu_q=0} = \sum_{p=1}^{\infty} c_p(T)\left(\frac{\mu_q}{T}\right)^p . \qquad (1)$$

The coefficients $c_p(T)$ are appropriate derivatives of the partition function with respect to μ_q and are evaluated at zero chemical potential. In [34] the series was truncated at fourth order. For comparison, one should recall that in the Stefan–Boltzmann limit the sixth order term vanishes at zero quark mass and is small at finite values. In Fig. 3 (left) the correction is plotted as a function of μ_q/T_0 where T_0 is the critical temperature at vanishing chemical potential. The correction rises steeply across the transition and peaks at about $1.1T_0$ before rapidly approaching the form $\Delta(p/T^4) = \alpha T^{-2}$ characteristic of the Stefan–Boltzmann limit, with the coefficient α having 82% of the continuum SB value. The comparison with the pressure at $\mu_q = 0$ [35] suggests that the correction gives a significant contribution at temperatures in the interval $[0.9\,T_0, 1.3\,T_0]$ and for $\mu_q/T_0 > 0.5$ only and decreases in importance as T rises further. To the right of Fig. 3 the quark number density n_q is shown which can be obtained similarly to Eq. (1). As μ_q increases, n_q rises steeply as the plasma phase is entered. Similar results have been obtained by [31, 33].

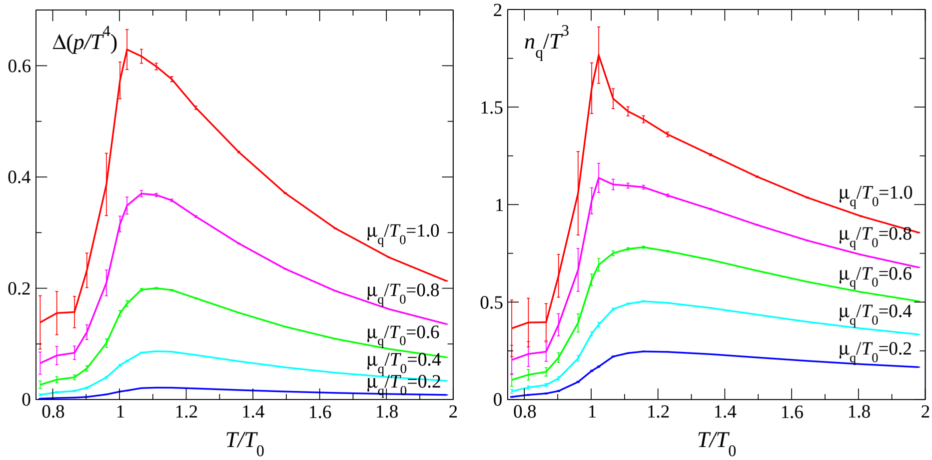

Fig. 3. The μ_q dependent contributions to the pressure (left) as a function of temperature at various values for the chemical potential. T_0 is the critical temperature at $\mu_q = 0$. To the right, the quark number density is shown. Both results are from [34].

As a by-product of the Taylor expansion approach one obtains results for susceptibilities [34] which are shown in Fig. 4. The susceptibilities are related to event-by-event fluctuations *e.g.* in charged particle multiplicities which have been proposed as signals for plasma formation [36]. The left figure contains results at vanishing chemical potential. Here χ_q denotes the quark number susceptibility, χ_I the isospin one and χ_C is the susceptibility for charge. For $T \leq T_0$ there is a significant difference between χ_q and χ_I, implying anti-correlated fluctuations of n_u and n_d. The difference decreases rapidly above T_0 and vanishes in the infinite temperature limit (denoted by the SB lines in the figure). Whether this difference is practically zero already at temperatures around, say, $2T_{\rm c}$ is currently being debated [31, 37, 38]. Finally, the right of Fig. 4 shows the quark number susceptibility for various values of μ_q. The peak which develops in χ_q when μ_q is increased is a sign that fluctuations in the baryon number density are growing as the critical end point in the (μ_q, T) plane is approached.

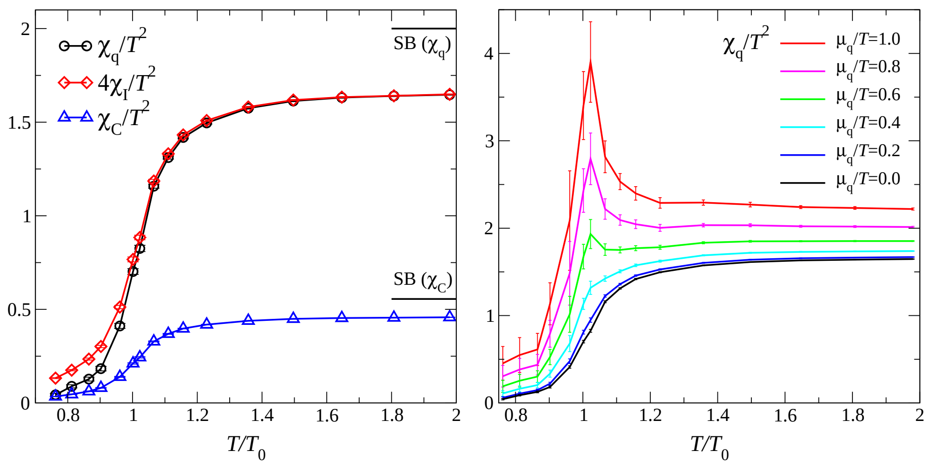

Fig. 4. Susceptibilities at vanishing chemical potential (left) and for various values of μ_q/T (from [34]).

3. Thermal hadron masses

Lattice simulations inevitably are carried out in Euclidean space-time. To make predictions for real-time processes, in general an analytic continuation to Minkowski space is necessary. At zero temperature, this is easy for particle masses and certain matrix elements. At finite temperature this is more complicated since *e.g.* the momentum space propagator is defined at discrete Matsubara frequencies $2\pi T n$ (for bosons) only. Moreover, Lorentz invariance is lost due to the presence of the heat bath causing, in general, differences between temporal and spatial correlators. Thus, lattice results for the more readily accessible screening masses can not immediately be used for the interpretation of experimental data. Temporal correlators, on the other hand, are hampered by the fact that the temporal extent of the system is physically limited by the inverse temperature which makes it difficult to isolate a ground state contribution normally dominating the correlators only at large distances.

The full information about the mere existence of plasma excitations and their properties as locations and widths eventually is contained in the spectral density $\sigma_H(p_0,\vec{p})$ for a channel with quantum numbers H. It is related to the temporal correlation function $G_H(\tau,\vec{p})$ at imaginary time τ as

$$G_H(\tau,\vec{p}) = \int\limits_0^{+\infty} \frac{dp_0}{2\pi}\sigma_H(p_0,\vec{p})\frac{\cosh[p_0(\tau-1/2T)]}{\sinh(p_0/2T)}\,. \qquad (2)$$

Ideally, by means of Eq. (2) one would like to extract the spectral density directly. Since the temporal correlation function is given as a discrete set of noisy data points only this is an ill-posed problem. Progress has been made recently [39] by applying the maximum entropy method (MEM) [40] which attempts to reconstruct the most likely spectral density, taking into account prior knowledge such as the perturbative behavior at large energies by means of a default model. The method has been successfully applied in various fields [40] and also recently in the context of zero temperature QCD where it was possible to disentangle the contributions of various excited states to a given correlation function [39, 41].

At temperatures above T_c it is of particular importance to be able to separate genuine (quasi-) particle contributions to σ_H from those arising from the free two-quark cut which are expected to dominate at very high temperatures also in the interacting case. For instance, in the pion channel, at zero quark mass, the free spectral density is given by ($p = |\vec{p}|$)

$$\begin{aligned}\sigma_\pi^{\mathrm{free}}(\omega,\vec{p},T) \;=\; & \frac{N_c}{8\pi^2}\left(\omega^2-p^2\right)\left\{\Theta\left(\omega^2-p^2\right)\frac{2T}{p}\ln\frac{\cosh(\frac{\omega+p}{4T})}{\cosh(\frac{\omega-p}{4T})}\right.\\ & \left. +\;\Theta(p^2-\omega^2)\left[\frac{2T}{p}\ln\frac{\cosh(\frac{p+\omega}{4T})}{\cosh(\frac{p-\omega}{4T})}-\frac{\omega}{p}\right]\right\}\,. \end{aligned} \tag{3}$$

It appears that MEM is capable of reproducing the free spectral density including the temperature effect in the infra-red as is shown in Fig. 5 (left): here, the free zero and non-zero temperature spectral densities are shown plus the output of a MEM analysis of a free continuum propagator at finite temperature [42].

On the other hand, one has to control the UV effects of the finite lattice cut-off. At the boundaries of the Brillouin zone energy bins are more densely populated before the amount of available momenta dies out [43]. This leads to the peaks shown to the right of Fig. 5 which move towards the continuum result with increasing lattice cut-off $1/a \sim N_\tau$.

Given these encouraging findings in the free case, one may lend some trust to the first results [44] for the vector channel finite temperature result at small quark mass shown in Fig. 6. The main features of the data are that the ρ peaks at temperatures below T_c, all computed at roughly the same physical quark mass, broaden with rising T and seem to disappear above T_c, changing to broad "resonance" like structures whose locations move proportional to the temperature. The vector spectral density is immediately related to a physical process, namely the cross section for the production of dilepton pairs. At vanishing momentum the relation reads

$$\left.\frac{dW}{dp_0 d^3p}\right|_{\vec{p}=0} = \frac{5\alpha^2}{27\pi^2}\frac{1}{p_0^2(\mathrm{e}^{p_0/T}-1)}\sigma_V(p_0,\vec{0})\;. \tag{4}$$

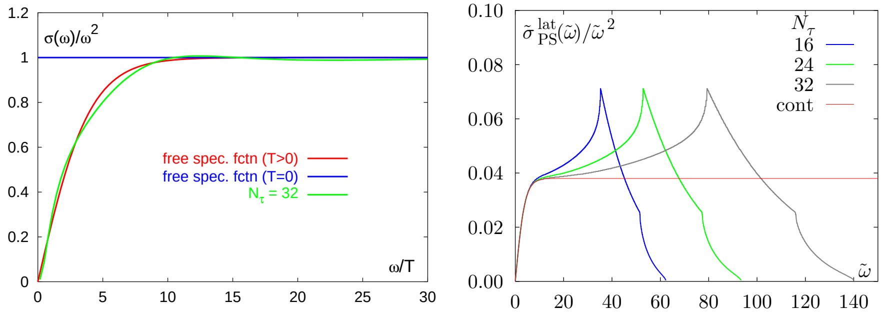

Fig. 5. Spectral densities for a pion made of free quarks. In the left plot densities (normalized to one) for $T = 0$ and $T > 0$ are compared to the MEM result obtained from the continuum propagator artificially discretized to 32 data points. The right plot compares (analytical) lattice densities at various lattice extents N_τ to the continuum one at $T > 0$ ($\tilde{\omega} = \omega/T$).

The rate is shown to the right of Fig. 6. The resonance-like enhancement of σ_V translates into the enhancement of the dilepton rate over the perturbative tree-level rate [45] for energies in the interval between $4T$ and $8T$. In contrast

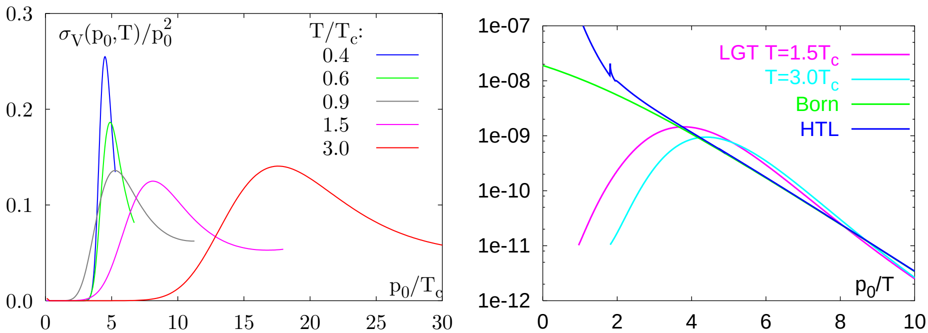

Fig. 6. Vector spectral densities at various temperatures (left). Below T_c the densities are given for roughly the same physical quark mass, above T_c the results are obtained very close to the chiral limit. To the right of the figure the corresponding dilepton rates, Eq. (4), at 1.5 and $3T_c$ are compared to the Born rate [45] and to the hard thermal loop result [46]. (From [44]).

to hard thermal loop calculations [46] where σ_V diverges at low energies, here the spectral density drops rapidly. From inspecting the correlation function it becomes clear already that σ_V vanishes $\sim p_0^\alpha$ with some power α in the $p_0 \to 0$ limit. Establishing in detail the behavior of spectral densities in the infrared, however, is rather difficult — for a first attempt see [47] — although it would be very interesting as the zero energy limit is related to transport coefficients [48] and thus to non-equilibrium properties.

4. Conclusion

The analysis of finite temperature QCD including dynamical quarks by means of numerical lattice simulations is steadily progressing. Moreover, I have reported on two big steps forward having been achieved by exploiting new techniques. There are first attempts to extract spectral densities in an unbiased way and first quantitative results are available now on QCD at small yet interesting values for the chemical potential. These include the critical temperature as well as the equation of state. None of the results has been obtained in the continuum limit yet but with new machines in the Teraflops range coming into operation soon, the systematic errors will be reduced and the analyses will be refined.

It is a great pleasure to thank Z. Burda and J. Jurkiewicz for the invitation to an inspiring workshop taking place in a marvelous atmosphere.

REFERENCES

[1] R.D. Pisarski, F. Wilczek, *Phys. Rev.* **D29**, 338 (1984).
[2] S. Gavin, A. Gocksch, R. Pisarski, *Phys. Rev.* **D49**, 3079 (1994).
[3] P. Vranas, *Nucl. Phys. B (Proc. Suppl.)* **83-84**, 414 (2000).
[4] F. Karsch, E. Laermann, *Phys. Rev.* **D50**, 6954 (1994); E. Laermann, *Nucl. Phys. Proc. Suppl.* **60**, 180 (1998) and references therein.
[5] S. Aoki *et al.* (JLQCD Coll.), *Phys. Rev.* **D57**, 3910 (1998).
[6] C. Bernard *et al.*, *Phys. Rev.* **D61**, 054503 (2000).
[7] S. Aoki *et al.*, *Nucl. Phys. Proc. Suppl.* **63**, 397 (1998).
[8] J. Engels *et al.*, *Phys. Lett.* **B514**, 299 (2001).
[9] See *e.g.* C. Gattringer *et al.*, `hep-lat/0209099` and references therein.
[10] F. Karsch, E. Laermann, Ch. Schmidt, *Phys. Lett.* **B520**, 41 (2001).
[11] X. Liao, *Nucl. Phys. Proc. Suppl.* **106**, 426 (2002).
[12] Ch. Schmidt, `hep-lat/0210037`.
[13] F.R. Brown *et al.*, *Phys. Rev. Lett.* **65**, 2491 (1990).
[14] S. Aoki *et al.*, *Nucl. Phys. Proc. Suppl.* **73**, 459 (1999).
[15] F. Karsch, E. Laermann, A. Peikert, *Nucl. Phys.* **B605**, 579 (2001).
[16] C. Bernard *et al.*, *Phys. Rev.* **D56**, 5584 (1997).
[17] A. Ali Khan *et al.*, *Phys. Rev.* **D63**, 34502 (2001).
[18] R.G. Edwards, U. Heller, *Phys. Lett.* **B462**, 132 (1999).
[19] N. Christ, private communication.
[20] S. Gupta, *Phys. Rev.* **D64**, 34507 (2001).
[21] For a review see I. Barbour *et al.*, *Nucl. Phys. Proc. Suppl.* **60**, 220 (1998).

[22] P. Braun-Munzinger *et al.*, *Phys. Lett.* **B518**, 41 (2001).

[23] Z. Fodor, S. Katz, *Phys. Lett.* **B534**, 87 (2002).

[24] Z. Fodor, S. Katz, *J. High Energy Phys.* **0203**, 14 (2002).

[25] P. de Forcrand, O. Philipsen, *Nucl. Phys.* **B642**, 290 (2002).

[26] M. D'Elia, M.-P. Lombardo, *Phys. Rev.* **D67**, 14505 (2003).

[27] A. Hart, M. Laine, O. Philipsen, *Phys. Lett.* **B505**, 141 (2001).

[28] S. Gottlieb *et al.*, *Phys. Rev.* **D38**, 2888 (1988).

[29] S. Choe *et al.*, *Phys. Rev.* **D65**, 54501 (2002).

[30] C. Allton *et al.*, *Phys. Rev.* **D66**, 74507 (2002).

[31] R.V. Gavai, S. Gupta, `hep-lat/0303013`.

[32] J. Cleymans, K. Redlich, *Phys. Rev.* **C60**, 54908 (1999).

[33] Z. Fodor, S. Katz, K.K. Szabo, `hep-lat/0208078`.

[34] C. Allton *et al.*, `hep-lat/0305007`.

[35] F. Karsch, E. Laermann, A. Peikert, *Phys. Lett.* **B478**, 447 (2000).

[36] S. Jeon, V. Koch, `hep-ph/0304012` and references therein.

[37] R.V. Gavai, S. Gupta, *Phys. Rev.* **D65**, 94515 (2002).

[38] J.-P. Blaizot, E. Iancu, A. Rebhan, *Phys. Lett.* **B523**, 143 (2001).

[39] M. Asakawa, T. Hatsuda, Y. Nakahara, *Phys. Rev.* **D60**, 91503 (1999); *Prog. Part. Nucl. Phys.* **46**, 459 (2001).

[40] R.K. Bryan, *Eur. Biophys. J.* **18**, 165 (1990).

[41] T. Yamazaki *et al.*, *Phys. Rev.* **D65**, 14501 (2002).

[42] F. Karsch, I. Wetzorke, Proceedings SEWM 2000, `hep-lat/0008008`.

[43] F. Karsch *et al.*, *Phys. Rev.* **D68**, 14504 (2003).

[44] F. Karsch *et al.*, *Phys. Lett.* **B530**, 147 (2002).

[45] J. Kapusta, *Phys. Lett.* **B136**, 201 (1984).

[46] E. Braaten, R.D. Pisarski, T. Yuan, *Phys. Rev. Lett.* **64**, 2242 (1990).

[47] S. Gupta, `hep-lat/0301006`.

[48] G. Aarts, J.M. Martinez Resco, *J. High Energy Phys.* **0204**, 53 (2002) and references therein.